Analysis of micro power generator autonomous PZT with use of sliding mode control

M. MEDDAD[a,c], A. EDDIAI[a, b], S. BELKHIAT[c], A. CHÉRIF[a, c], A. HAJJAJI[d],
S. BENAHDOUGA[c], Z. SASSI[e], S. TOUHTOUH[d]
aLaboratoire de Génie Electrique et Ferroélectricité, LGEF, INSA Lyon, Bat. Gustave Ferrie, 69621 Villeurbanne Cedex, France
bLaboratoire de Physique de la Matière Condensée, Faculté des Sciences, Université Chouaib Doukkali, El Jadida, Morocco
cLaboratoire DAC HR, Université Ferhat Abbas, 19000, Sétif, Algéria.
dEcole Nationale des Sciences Appliquées, Université Chouaib Doukkali, El Jadida, Morocco
eUniversity Claude Bernard Lyon1, France

Research on energy harvesting and related technologies have attracted attention and have shown their potential in a wide range of applications, the portable electronic devices (numerical telephones, diaries, microcomputers, watches, medical prostheses…) accompany us, often in a banal way, in the everyday life; they render very many services to us but, because of their insufficient autonomy, also force us in our desires of mobility and autonomy.Many mechanisms of energy conversion and device designs for vibration-based energy harvesting have been developed and reported in literature, In addition to electromagnetic and electrostatic mechanisms that have been widely applied, many other mechanisms such as electrostrictive and dielectric polymers have also been investigated . The power optimality performance of a piezoelectric energy harvester connected to a resistive load is studied. An analytical solution for the piezoelectric energy harvester based on the piezoelectric constitutive equations and the fundamental mechanics of materials relations is adapted to estimate the optimal power and vibration amplitude. The influence of geometrical parameter on the stack piezoelectric is also investigated. The power harvesting in a pressure-loaded plate depends on several factors. The dominant parameters that affect the performance are the ratio of thickness layer and the area of electrode, a designated power management module for sub mW energy harvester is proposed in this article to increase the energy conversion efficiency and extend the energy storage Life time for small input power, with use sliding mode control The specimen was simulate under tow values ratio of thickness layer and the area 1/0.09 and 0.1/0.01. The measured output voltages for two different ration is 8V and The results indicate that the electricity power output has 2.2 mW.

1. Introduction

Numerous industrial and military applications require remote sensing of various machine and equipment operating parameters in locations where traditional power sources may not be available and long periods of unattended operation are required [1]. Mechanical vibration energy can be converted into electrical energy using piezoelectric power generator. The electrical energy is usually collected by storage [2]. The reduction in the consumption of the electronic components allowed the rise of mobile applications without wire. The batteries, which initially supported the development of portable electronic instruments, paradoxically became a barrier to this progression, in particular because of the associated problems of maintenance (refill, replacement). To avoid the use of the reserves of energy with limited capacities, one can benefit from the Considerable reduction in consumption in energy of various electronic devices. It is now possible to feed an electronic system starting from a source of ambient energy (energy present in the environment of dispositive) [3]. The human body stores, dissipates and develops a considerable energy compared to the consumption of the majority of the portable electronic devices. It thus seems possible to recover part of this energy to feed from the apparatuses of power moderated [4].detail the potential sources of energy of the human body.The mechanical power developed at the time of simple muscular activities such as going (67W), turning a crank (21W), to tighten with the hand (6W), etc is compared with the consumption of some current portable electrical appliance, like small a radio operator FM (30mW), a Walkman (60mW) or a portable telephone (35mW in communication).This comparison justifies the idea to create generating devices of energy which make it possible to create electric power starting from a voluntary and specific movement of the user. Several examples of achievements practice are quoted; one of the potential biomedical applications of piezoelectric generators is in implantable drug delivery systems, An interesting preliminary concept has been demonstrated such as a self-powered system using a nano-power-generator for long

distance wireless data transmission [5] Multimodal energy harvesting is one strategy widely pursued for broadband purpose [6-11]. This paper aims at studying the effect of the geometrical parameter on the optimal power outputs, and an alternative approach is to use a piezoelectric generator to recharge and/or power drug delivery systems with use sliding mode control.

2. Principle

The piezoelectric microphone-generators are based on the direct effect of piezoelectricity, namely that the application of pressure on an electrode piezoelectric material involves the appearance of a voltage between the electrodes. The piezoelectric generators can consist of a mechanical system presenting a frequency of resonance which couples the generator with the ambient vibrations or the piezoelectric elements can be directly requested. In a general way a piezoelectric microgenerator Fig.1, consists of a mechanical device able to transmit a mechanical request to a piezoelectric element , itself connected to an electric circuit constituting the receiver of energy. The potential difference between the final electrodes of the piezoelectric element depends primarily on the mechanical request and the behavior of the electric charge. The piezoelectric system (PZT) fig 2 is the central body of electric conversion mechanical.It is a "sandwich" of piezoelectric thin layers. The mechanical device of application (DMA) allows the purely mechanical conversion of the force F delivered by the mechanical source into another force F of form and amplitude adapted to the PZT. This device makes it possible to transform a limited effort of weak frequency into a constraint of higher frequency and stronger amplitude. The system of storage (S.S) fig 3 is a static inverter. It makes it possible to convert the energy (rough) delivered by PZT into energy usable by the targeted portable apparatus, or possibly in energy stored in an element of type the condensing or accumulating electrochemical
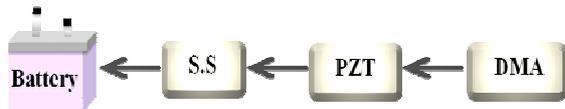

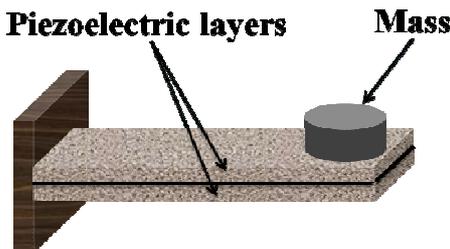*Fig.1. Diagram synoptic of the generator power harvesting.*

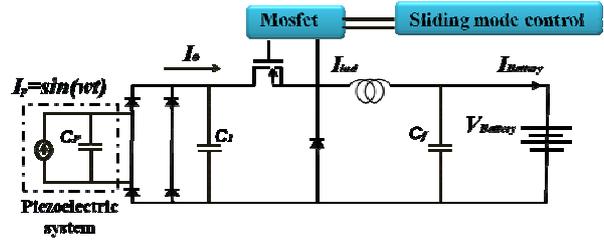*Fig.2. Principle of the mechanical device of application.*

Fig.3. Electronic system of stockade [14].

3. Modeling

The piezoelectric ceramics subjected to a constraint electrically becomes polarized (Fig.4).
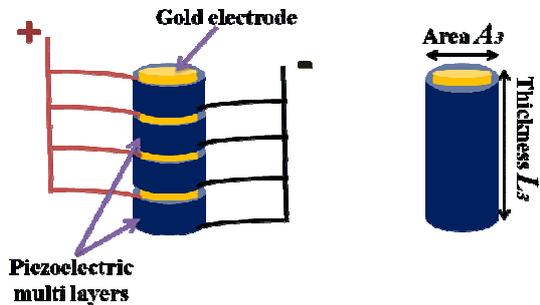

Fig.4. Section of a piezoelectric with multi layers.

The system is composed of a beam on which thin piezoelectric layers are deposited. Let us point out the starting equations (1). These resonant models are established starting from the static equations of the piezoelectricity, to which the law of Newton is added. For example, for a long bar functioning in mode 33 [12]:

$$\begin{cases} S_3 = s_{33}^D . T_3 + g_{33} . D_3 \\ E_3 = - g_{33} . T_3 + \beta_{33}^T . D_3 \end{cases} \quad (1)$$

Where S_3 is the strain, s_{33} is the compliance, T_3 is the stress, g_{33}, β_{33} is the piezoelectric coefficients, E_3 is the electric-field vector, D_3 is the electric displacement vector, and ε_{33} is the permittivity.
With the law of Newton:

$$\frac{\partial T_3}{\partial x_3} = - \rho . \frac{\partial^2 . u}{\partial t^2} \quad (2)$$

$$\frac{\partial^2 u}{\partial x_3} = \rho . s_{33}^D . \frac{\partial^2 u}{\partial . t^2} \quad (3)$$

This equation corresponds, in sinusoidal mode, with a vague mechanics of propagation; the equivalent circuit of Masson is composed of three parts: the mechanical branch, the electric branch and a transformer which symbolizes

electromechanical conversion. The mechanical branch of the circuit is described by the system [13]

$$\begin{cases} F_1 - f = Z_1(j\omega)(V_1 - V_2) + Z_2(j\omega).V_1 \\ F_2 - f = Z_1(j\omega).(V_1 - V_2) - Z_2(j\omega).V_2 \end{cases} \quad (4)$$

With F_1, F_2, V_1 et V_2 are respectively the forces and speeds at the ends of the bar, Z_1, Z_2 the impedance mechanics and F the force due to piezoelectricity.
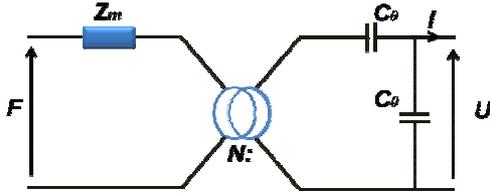

Fig.5. Electromechanical circuit equivalent.

Since the piezoelectric bar used in our application is inserted at an end, V_2 speed $= 0$, which simplifies I the equivalent circuit (fig.5) obtained with the new system of equations:

$$\begin{cases} Z(j\omega).V_1 = N.\dfrac{1}{j.C_0} + F \\ I = N.V_1 - jC_0.\omega.U = \dfrac{U}{R_l} \end{cases} \quad (5)$$

With Z the mechanical impedance this one represents can be linearized in the vicinity of the frequency of resonance by

$$Z(j\omega) = jL_m.\omega + \frac{1}{jC_m\omega} + R_m \quad (6)$$

With the development of the equations one can easily deduce the following equations in the field frequential:

$$\frac{du}{dx_3} = -p \frac{s_{33}^D}{A_3} \left(F - \frac{g_{33}}{s_{33}^D}.\frac{I}{p} \right) \quad (7)$$

$$\frac{d}{dx_3} \left(F - \frac{g_{33}}{s_{33}^D}.\frac{I}{p} \right) = -\rho A_3.p.u \quad (8)$$

As well as the coefficient of conversion N to represent by the expression $N = \dfrac{g_{33}}{s_{33}^D} C_0$.

One can deduce the following equations easily:

$$\begin{cases} Z(j\omega).V_1 = N.\dfrac{1}{jC_0.\omega} + F \\ I = N.V_1 - jC_0\omega.U = \dfrac{U}{R_l} \end{cases} \quad (9)$$

The development of this system makes it possible to easily deduce the analytical model from a piezoelectric system in dynamic mode

$$\begin{cases} U = \dfrac{R_L.N.\dfrac{1}{jC_0\omega}.F}{(R_L + \dfrac{1}{j.C_0})Z(j\omega) + \dfrac{h_{33}^2}{\omega^2}} \\[4mm] I = \dfrac{N.\dfrac{1}{jC_0\omega}.F}{R_L + (\dfrac{1}{jC_0\omega})Z(j\omega) + \dfrac{h_{33}^2}{\omega^2}} \\[4mm] V_1 = \dfrac{R_L + \dfrac{1}{JC_0\omega}}{(R_L + \dfrac{1}{jC_0\omega})Z(j\omega) + \dfrac{h_{33}^2}{\omega^2}} \end{cases} \quad 10)$$

4. Storage systems

The system of recovery associated with the piezoelectric system plays a significant role. Generated energy is not in general directly usable by the targeted portable device. The power recovered in the piezoelectric microgenerateurs depends closely on the electromechanical coupling. One of the techniques of conversion with amplification of delivered energy was proposed per G K Ottman et al. [14], which initially developed it to damp out the sinusoidal vibrations of a vibrating structure, using piezoelectric patches positioned on the structure. This method is used to optimize the maximum power transferred towards the battery with the use of a DC-DC converter. And a chart DSP to generate a signal PWM with use of proposed technique sliding mode control. The piezoelectric elements as well as the variable checking circuit structure are represented on fig.6:

$$\int_0^{t_d} I_p.\sin(wt).\partial(wt) = w.C_p.(v_p(t_d) - v_p(0)) \quad (11)$$

$$\cos(wt_d) = 1 - \frac{2.V_1.w.C_p}{I_p} \quad (12)$$

In the interval of time $wt_d < wt < T$, the outgoing current of the bridge of rectifier can be calculated starting from the relation:

$$I_0(t) = \frac{C_1}{C_1 + C_p} I_p(t) \qquad (13)$$

Or the power on the outlet side of the rectifier is:

$$\langle P(t) \rangle = \frac{2.V_1}{\pi}.(I_p - V_1.w.C_p) \qquad (14)$$

I_p the current delivered by the piezoelectric source

5. Sliding mode control
The state equations of our linearized system are: [10]

$$\dot{Z}_i = A_i.Z_i + B_i.V_i + B_{pi}w_i \qquad (15)$$

$$Y_{1i} = C_i Z_{1i}$$

Where $i = 1,2,3$ *and* $Z_i = [\; Z_{1i} \;\; Z_{2i} \;\; Z_{3i} \;]^T$ *is the new state vector.*

$$A_i = \begin{bmatrix} 0 & 1 & 0 \\ 0 & 0 & 1 \\ 0 & 0 & 0 \end{bmatrix}$$

The vectors B_i, B_{pi}, C_i *and the matrix* A_i *are given by:*

$$B_{pi} = \begin{bmatrix} 0 \\ 0 \\ 1 \end{bmatrix} \quad B_i = \begin{bmatrix} 0 \\ 0 \\ 1 \end{bmatrix}$$

$$C_i = \begin{bmatrix} 1 & 0 & 0 \end{bmatrix}$$

The first step in sliding mode controller conception it's the chose of commutation surface. The commutation surface is defined by:

$$S_i(z) = \begin{bmatrix} K_{1i} & K_{2i} & K_{3i} \end{bmatrix} \cdot \begin{bmatrix} Z_{1i} \\ Z_{2i} \\ Z_{3i} \end{bmatrix} + K_{1i}W_i = 0 \quad (16)$$

After this we calculate the states feedback vector K_i *by using the pole placement method.* W_i *is the reference = constant*

The equivalent control V_{eqi} *is calculated by:*

$$\dot{S}_i = 0 \quad \Leftrightarrow \quad K_i \dot{Z}_i + K_{1i} \dot{W}_i = 0 \,(17)$$

$$\Rightarrow V_{eqi} = -[K_i B_i]^{-1} K_i A_i Z_i - [K_i B_i]^{-1} K_i B_p w_i$$

Replace V_{eqi}

$$\dot{Z}_{eqi} = \left[A_i - B_i[K_iB_i]^{-1}K_iA_i\right]Z_i + \left[I - B_i[K_iB_i]^{-1}K_i\right]B_pw_i \quad (18)$$

$$A_{eqi} = \left[A_i - B_i[K_iB_i]^{-1}K_iA_i\right] \qquad (19)$$

A_{eqi} it's a dynamic matrix of equivalent system

$$A_{eq} = \begin{bmatrix} 0 & 1 & 0 \\ 0 & 0 & 1 \\ 0 & -K_{1i}/K_{3i} & -K_{2i}/K_{3i} \end{bmatrix}$$

The characteristic polynomial is the following:

$$P_i(\lambda) = \lambda_i\left[\; \lambda_i^2 + (K_{2i}/K_{3i}\;)\lambda_i + K_{1i}/K_{3i} \;\right] \qquad (20)$$

We choose the following poles:
$-\rho_t + j\rho_t$ *and* $-\rho_t - j\rho_t$ *imply, that's the constant gain is directly determined according to the choice of this poles.*

$$K_{3i} = 1$$
$$K_{1i} = 2\rho_i$$
$$K_{2i} = 2\rho_i^2$$

Finally the feedback vector K_i *is given by:*

$$K_i = \begin{bmatrix} 2.\rho_i^2 & 2.\rho_i & 1 \end{bmatrix} \qquad (21)$$

The commutation surface is written:

$$S_i(z) = \begin{bmatrix} 2.\rho_i^2 & 2.\rho_i & 1 \end{bmatrix} \cdot \begin{bmatrix} Z_{1i} \\ Z_{2i} \\ Z_{3i} \end{bmatrix} + K_iW$$

The following step is to calculate the sliding mode control law.

$$v_i(Z) = V_{eqi} - g_i sign(s_i) \qquad (22)$$

6. Simulation

The model of the system shows well that their equivalent circuits are similar, it is consisted a mechanical branch represented by a resounding impedance Z(W), a transformer and an impedance representing electromechanical conversion. With bars piezoelectric of **P188 types** and the sizes of the following table

Table1. Parameters used for simulation

Characteristic	Parameter
$\rho = 7700 kg/m^3$	$C_0 = 6.64 \times 10^{-12}\,F$
$s_{33}^D = 9.09 \times 10^{-12}\,m^2/N$	$N = hC_0 = 0.09$
$g_{33} = 26 \times 10^{-3}\,Vm/N$	$C_m = 8.19 \times 10^{-9}\,F$
$h_{33} = 28.6 \times 10^8\,V/m$	$L_m = 3.47 \times 10^{-4}\,H$
$\beta_{33}^T = 6.11 \times 10^7\,V^2/N$	$R_m = 16.2\,\Omega$
$Q_m = 80$	$G_0 = 23.4$
$L_3 = 1 cm$	$\zeta = 0.039$
$A_3 = (3mm)^2$	

We have modeled an energy harvesting generator based on the use of piezoelectric unimorph diaphragm and multilayer structure operating in flexion mode. A maximum voltage of 8V was generated under a force of 55m N and a resonance frequency of the harvester is about 10^5 Hz for unimorph structure and 10^6 Hz for multilayer structure Fig. 6.
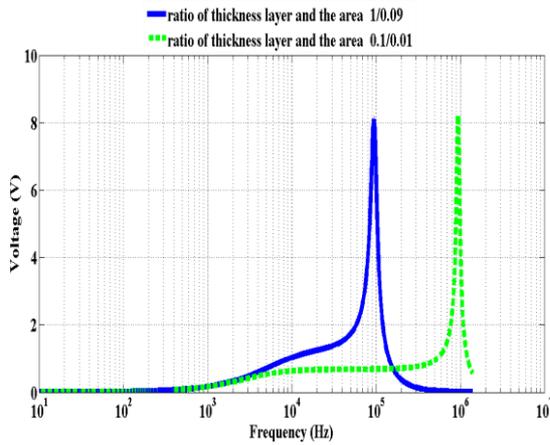

Fig.6. Voltage generated according to the frequency.

Fig.7 shows the results of the harvester output voltage with various resistive. It was measured with a fixed pre-stress condition of 55m N, this figure illustrates that the output voltage raise as the impedance of the resistor increases for the tow structure. When the resistance is 100 kohm the maximum voltage approaches 8V. Fig. 8 shows that a maximum output power of about 2.2 mW generated with resistive load 105Kohm. There is the maximum power output when the efficiency corresponds to a value of 0.42.
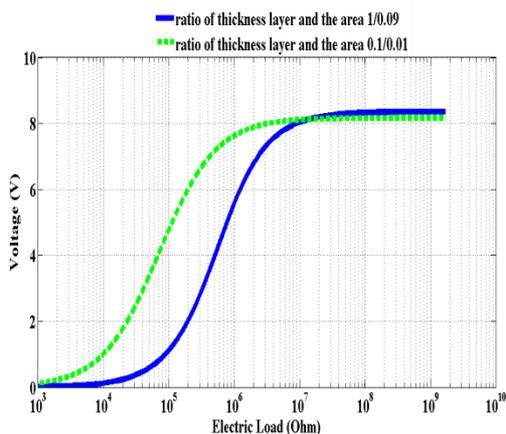

Fig.7. Voltage generated according to the electric load..
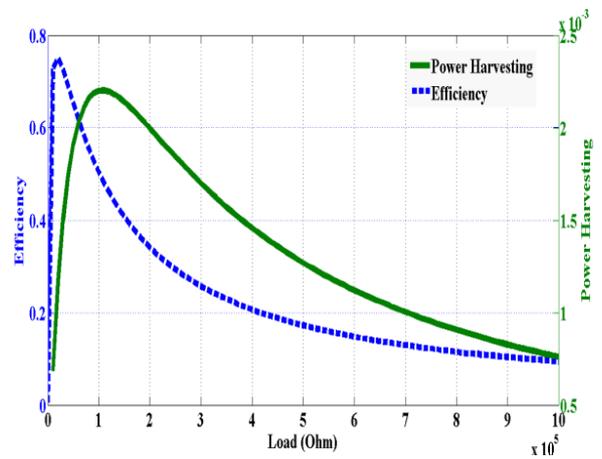

Fig.8. Power harvesting output and Efficiency according to the load with report/ratio Thicknesses/Area = 1/0.09.

The next step was performed to validate the energy transfer to the storage battery. According to the theory presented in section IV, the difference between the last step resides in an added electrical electronic circuit with the use sliding mode control. Fig. 9 and Fig. 10 present the power and Battery current versus cyclic ratio. This data displays the existence of an optimal cyclic ratio of 3% for a maximum transfer of energy to the storage battery. For the proposed configuration (multilayer configuration, on the other hand, the maximum power reached a value of 2.2mw with an optimal load resistance of 1MΩ. The magnification made it possible to see that the proposed configuration multilayer structure clearly demonstrated an output power increase that was 80% greater as compared to the standard technique,
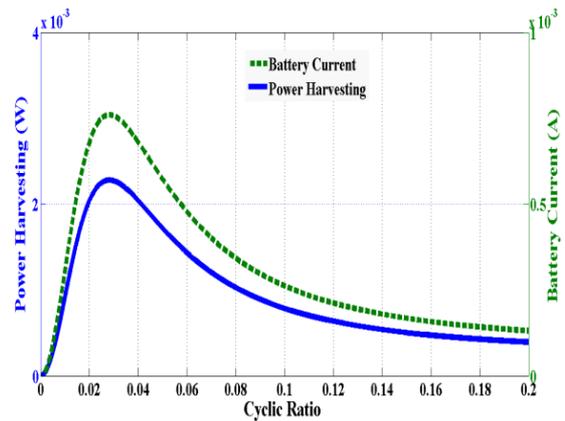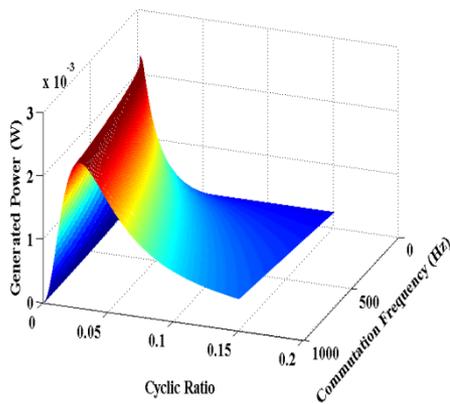

Fig.9. Power Harvesting according to the cyclic ratio.

*Fig.10. Power Harvesting according to the cyclic ratio
and the frequency of commutation.*

When the tension of Vs source varied from 40 flight towards 30 flight (with T = 0.2 Vs = 30). It is noticed that the order is robust compared to the variation of the tension of Vs source.
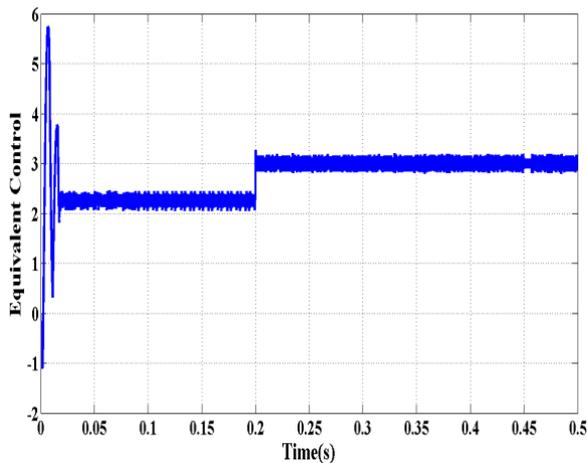

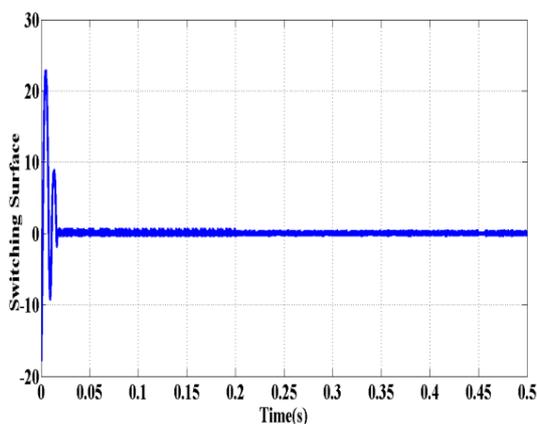*Fig.11. Primary voltage of the chopper according the frequency*

Fig.12. Sliding mode control robustness

6. Conclusions

This article proposes an application approach for increasing the conversion abilities of piezoelectric structure According to Fig.6 and Fig.7 one notices well that the generated voltage reached the same value for both geometry different thickness and surface from a piezoelectric bar but all keep of it almost the same ratio (thickness /Area) for the goal to maintain a voltage raised with a bar to constitute N layers for a bar thickness 1çm and surfaces the 0.09 cm^2 voltage to generate and the same one with a layer thickness 0.1çm and surfaces 0.01cm^2 my with two different frequency of resonance. Analysis the simulation results of this study enabled us to confirm the advantage of using the layers piezoelectric for the design of a micro power generator based on a ceramics PZT, it shows well that with layers 10x0.1çm the power reaches a maximum of 2.2mw through the maintenance voltage to raise it by the order in sliding mode and the maximization of the current induces has through the layers to connect in parallel.

References

[1] M. P. Buric. IEEE transactions one power electronics, 1-5 (2006).
[2] J. Lin. IEEE transactions one power electronics; 2464–2467 (2008).
[3] M. Marzencki. Doctoral thesis University TIMA Laboratory fourier Josephus (2008).
[4] S. Turri and G. Poulin. Days Electrotechnical Club EEA, Cachan, France (2002).
[5] Y. Hu, Y. Zhang, C. Xu, L. Lin, R. L. Snyder, Z. L. Wang. Nano Lett, **11**(6), 2572 (2011).
[6] Q. Ou, X. Q. Chen, S. Gutschmidt, A. Wood, N. Leigh, and A. F. Arrieta. J. Intell. Mater. Syst. Struct, **23**, 117 (2012).
[7] M. Arafa, W. Akl, A. Aladwani, O. Aldrarihem, A. Baz. Proc. SPIE, **7977**, 79770Q (2011).
[8] A. Erturk, J. M. Renno, D. J. Inman. J. Intell. Mater. Syst. Struct. March, **20**, 529-544 (2009).
[9] H. Wu, L. H. Tang, Y. W. Yang, C. K. Soh. Jpn. J. Appl. Phys., Part 1 51, 040211 (2012).
[10] I.-H. Kim, H.-J. Jung, B. M. Lee, S.-J. Jang. Appl. Phys. Lett., **98**, 214102 (2011).
[11] L. H. Tang, Y. W. Yang. J. Intell. Mater. Syst. Struct. **23**, 1627 (2012).
[12] Stephen R. Platt, F. Shame, H. Hani. IEEE/ASME Transaction one mechatronics, Flight **10**, 240 (2005).
[13] G. Poulin. University bets XI thesis of doctorate juin (2004).
[14] G. K. Ottman, H. F. Hofmannn, A. C. Bhatt, G. A. Lesieutre. IEEE transactions one power electronics, **18**, 696 (2003).

*Corresponding authors: m_meddad@yahoo.fr;
aeddiai@gmail.com